Penetration and Accumulation of Dendrons with Different Peripheral Composition in Pseudomonas aeruginosa Biofilms

Rozenbaum, Rene T; Andrén, Oliver C J; Van der Mei, Henny C; Woudstra, Willem; Busscher, Henk J; Malkoch, Michael; Sharma, Prashant Kumar

Published in:
Nano Letters

DOI:
10.1021/acs.nanolett.9b00838

Publication date:
2019

NANO LETTERS

Letter

Cite This: Nano Lett. XXXX, XXX, XXX−XXX

pubs.acs.org/NanoLett

Penetration and Accumulation of Dendrons with Different Peripheral Composition in *Pseudomonas aeruginosa* Biofilms

René T. Rozenbaum,[†] Oliver C. J. Andrén,[‡] Henny C. van der Mei,[†] Willem W. Woudstra,[†] Henk J. Busscher,[†] Michael Malkoch,*[,‡] and Prashant K. Sharma*[,†]

[†]Department of Biomedical Engineering, University of Groningen and University Medical Center Groningen, P.O. Box 196, 9700 AD, Groningen, The Netherlands

[‡]Department of Fibre and Polymer Technology, KTH Royal Institute of Technology, 10044 Stockholm, Sweden

Supporting Information

ABSTRACT: Multidrug resistant bacterial infections threaten to become the number one cause of death by the year 2050. Development of antimicrobial dendritic polymers is considered promising as an alternative infection control strategy. For antimicrobial dendritic polymers to effectively kill bacteria residing in infectious biofilms, they have to penetrate and accumulate deep into biofilms. Biofilms are often recalcitrant to antimicrobial penetration and accumulation. Therefore, this work aims to determine the role of compact dendrons with different peripheral composition in their penetration into *Pseudomonas aeruginosa* biofilms. Red fluorescently labeled dendrons with pH-responsive NH_3^+ peripheral groups initially penetrated faster from a buffer suspension at pH 7.0 into the acidic environment of *P. aeruginosa* biofilms than dendrons with OH or COO^- groups at their periphery. In addition, dendrons with NH_3^+ peripheral groups accumulated near the top of the biofilm due to electrostatic double-layer attraction with negatively charged biofilm components. However, accumulation of dendrons with OH and COO^- peripheral groups was more evenly distributed across the depth of the biofilms than NH_3^+ composed dendrons and exceeded accumulation of NH_3^+ composed dendrons after 10 min of exposure. Unlike dendrons with NH_3^+ groups at their periphery, dendrons with OH or COO^- peripheral groups, lacking strong electrostatic double-layer attraction with biofilm components, were largely washed-out during exposure to PBS without dendrons. Thus, penetration and accumulation of dendrons into biofilms is controlled by their peripheral composition through electrostatic double-layer interactions, which is an important finding for the further development of new antimicrobial or antimicrobial-carrying dendritic polymers.

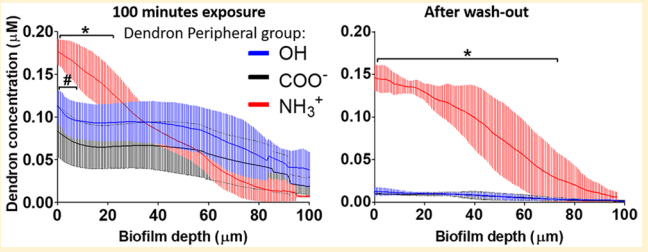

KEYWORDS: *Nanomedicine, nanocarriers, nanotechnology, dendrimers, dendritic polymers*

Biofilms are three-dimensional microbial aggregates responsible for 60−80% of all microbial infections.[1] In an infectious biofilm, infecting organisms are protected by a matrix of self-produced extracellular polymeric substances (EPS), impeding effective penetration of most antimicrobials.[2] This protection mechanism was already observed in 1684 by Antonie van Leeuwenhoek, describing how the vinegar which he used to wash his teeth only killed those bacteria which were on the outside of the scurf,[3] nowadays called "biofilm". To date, with the threat of antimicrobial-resistant bacterial infection becoming the number one cause of death by the year 2050,[4] effective penetration of antimicrobials into biofilms is still a major hurdle in the treatment of infectious biofilms.

Dendritic polymers with dendrimers as the flagship are flawless and symmetrically branched macromolecules with a treelike structure.[5] When composed of antimicrobial peptides,[6,7] such dendrimers are able to kill planktonic bacteria,[6] that is, suspended bacteria that are not in their protected, adhering, biofilm-mode of growth. Also antimicrobial dendrimers can prevent biofilm formation.[7] For the treatment of existing infectious biofilms, dendrimers are under investigation for use as an antimicrobial nanocarrier.[5] Vancomycin-tethered poly(amidoamine) dendrimers showed avid binding to vancomycin-resistant *Staphylococcus aureus* surfaces.[8] However, it is unclear whether the peripheral composition of dendritic nanocarriers stimulating avid binding to biofilm inhabitants is favorable or not for their deep penetration into an infectious biofilm. Dendrons are wedge-shaped structures that are the major component of dendrimers.[9] These dendritic frameworks are inherently bifunctional containing one chemically addressable group designated to the focal point and a composition of multiple peripheral groups. Higher generation dendrons are by definition dendrimers with an active core and therewith the chemical composition of larger dendrons, similar to

Received: February 26, 2019
Revised: May 28, 2019
Published: May 30, 2019

DOI: 10.1021/acs.nanolett.9b00838
Nano Lett. XXXX, XXX, XXX−XXX

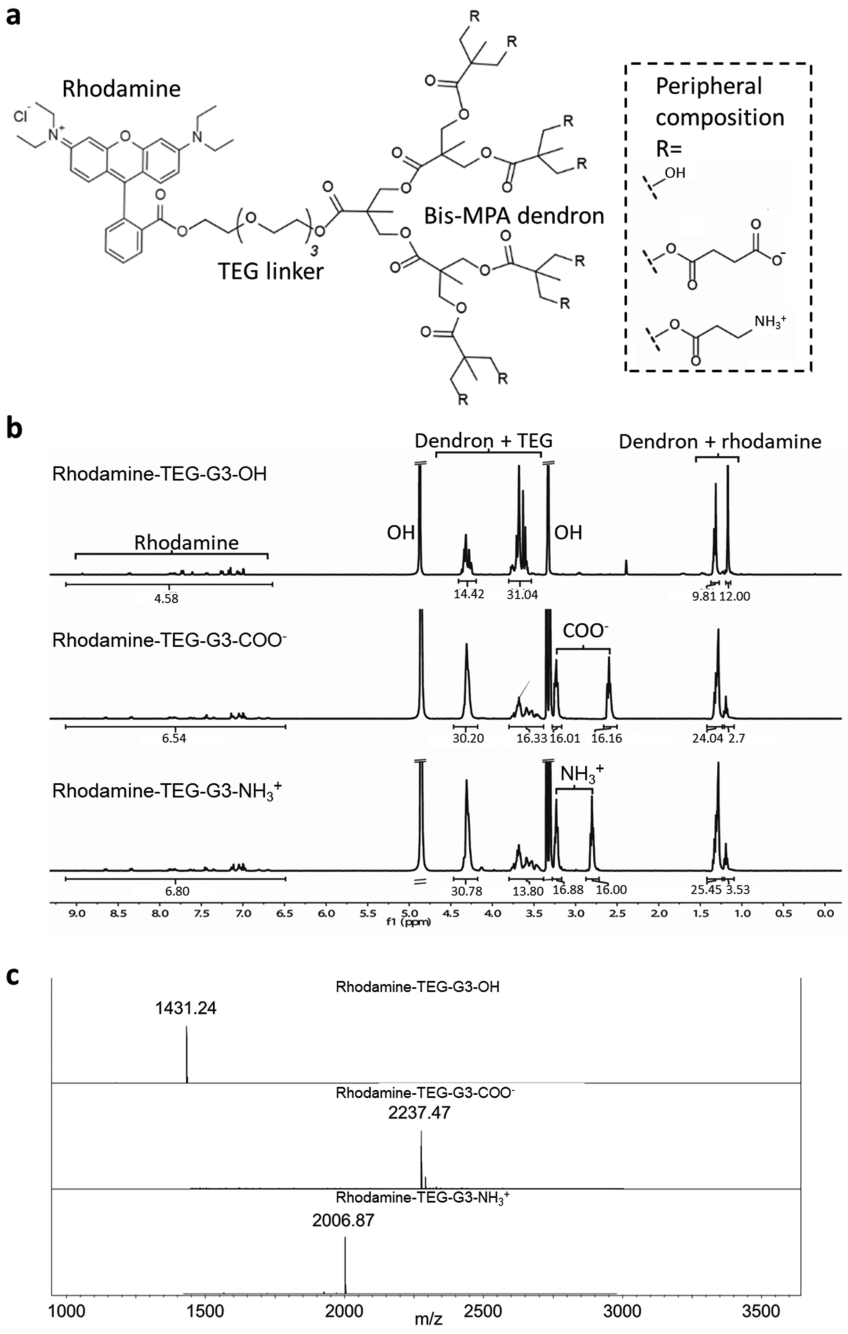

Figure 1. (a) Bifunctional dendrons displaying different pH-responsive peripheral composition, consisting of fluorescent marker (rhodamine B), an unsymmetrical TEG linker, and three generations (G3), multivalent bis-MPA dendrons. Charges indicated are as in the acidic environment of a biofilm. (b) ^{1}H NMR of TEG-G3-OH, rhodamine-TEG-G3-COO^{-}, and rhodamine-TEG-G3-NH$_3^{+}$. ^{1}H NMR analyses were performed as described previously,[15] using a Brüker AM NMR (Brüker Biospin, Rheinstetten, Germany). (c) MALDI-TOF-MS of rhodamine-TEG-G3-OH, rhodamine-TEG-G3-COO^{-}, and rhodamine-TEG-G3-NH$_3^{+}$. MALDI-TOF spectra were obtained as described previously,[15] using a Brüker UltraFlex MALDI-TOF MS with SCOUT-MTP Ion Source (Brüker Daltonics, Bremen, Germany), a gridless ion source with the nitrogen-laser (337 nm) and a reflector. .

dendrimers, is responsible for efficient penetration in infectious biofilms.

Considering the importance of penetration and accumulation of antimicrobials into an infectious biofilm and the promise of dendrimer-based antimicrobials for infection control, this work aims to determine the role of dendron peripheral composition in their penetration into *Pseudomonas aeruginosa* biofilms. *P. aeruginosa* causes a range of infections across the human body[10] and is known to produce extensive amounts of EPS that can be especially troublesome in cystic fibrosis patients.[2] Better understanding of the role of peripheral composition of dendrons in their penetration and accumulation into biofilm will aid their further development as an effective antimicrobial.

To this end, bifunctional dendrons were designed, consisting of rhodamine B as a red-fluorescent marker, an unsymmetrical triethylene glycol (TEG) linker, and three-generations (G3), multivalent 2,2-bis(hydroxymethyl)propionic acid (bis-MPA)

DOI: 10.1021/acs.nanolett.9b00838
Nano Lett. XXXX, XXX, XXX−XXX

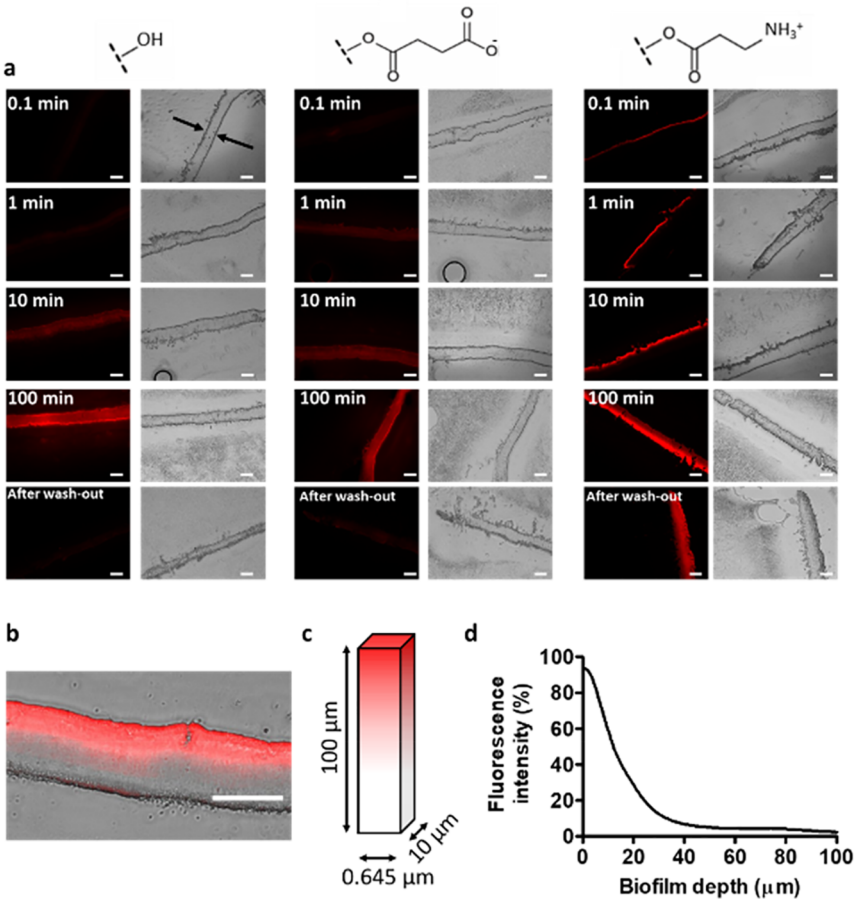

Figure 2. (a) Cross-sectional images of *P. aeruginosa* biofilms exposed to 0.2 μM dendron suspensions in PBS with different peripheral composition for 0.1, 1, 10, or 100 min and after 100 min wash-out in PBS (initial exposure time to dendron suspensions: 100 min). Identical alignment of the biofilms after embedding and cryo-sectioning was impossible, hence each fluorescence image is complemented with a light-microscopic image to visualize the entire biofilm (grasped within two arrows in the second image from the left, top row). The white scale bar represents 100 μm. (b) Enlarged overlayer of fluorescence and light-micrographs of dendrons accumulated in a biofilm. Scale bar represents 100 μm. (c) A custom LabVIEW script was used to calculate the fluorescence intensity in a 10 × 0.645 μm (corresponding with one pixel) biofilm column as a function of biofilm depth (see also Experimental Section). (d) Example of fluorescence intensity as a function of biofilm depth, calculated as described in panel c, from which the depth-dependent dendron concentration was derived, using a standard curve (Figure S2).

dendrons. Bis-MPA dendrons are biocompatible[11] and biodegradable[12] and can be synthesized with unprecedented structural control.[13] Three different dendrons with pH-responsive peripheral composition were synthesized (see Figure 1a): rhodamine-TEG-G3-OH, rhodamine-TEG-G3-COO^-, and rhodamine-TEG-G3-NH_3^+ (charges indicated are as in the acidic environment inside a biofilm). Dendrons were constructed using conventional divergent growth of bis-MPA.[14,15] Rhodamine B was covalently attached through fluoride-promoted esterification (FPE) chemistry and the peripheral hydroxyls were activated yielding the neutral dendritic scaffold, rhodamine-TEG-G3-OH. Esterification of rhodamine-TEG-G3-OH yielded anionic rhodamine-TEG-G3-COO^- and cationic rhodamine-TEG-G3-NH_3^+ (see Supporting Information for details).[14−16] Complete substitution and high structural purity were corroborated using conventional characterization techniques for dendrimer chemistry, that is, NMR (Figure 1b) and MALDI-TOF-MS (Figure 1c).

Next, *P. aeruginosa* ATCC 39324 biofilms were grown in a constant depth film fermenter (CDFF)[17] to a thickness of 100 μm, as verified using optical coherence tomography (OCT result: 96 ± 15 μm, averaged across all biofilms employed in this study). Biofilms were exposed to red-fluorescently labeled dendron suspensions for 0.1, 1, 10, or 100 min to study their penetration. In addition, biofilms after 100 min of exposure to a dendron suspension in phosphate buffered saline (PBS, pH 7.0) were subsequently placed in PBS without dendrons for another 100 min to monitor dendron wash-out. Note that in a separate experiment (data not shown), it was established that dendrons did not inadvertently release covalently coupled rhodamine in buffer, regardless of pH. After penetration and/or wash-out, biofilms were immediately embedded into Tissue-Tek O.C.T. compound and flash-frozen in liquid nitrogen after which 10 μm sections were made perpendicular to the biofilm surface using a cryotome (Leica CM3050 S, Leica Microsystems, Wetzlar, Germany) for fluorescence microscopy. Figure 2a,b shows examples of cross-sectional images of biofilms after exposure to the different dendron suspensions at different time points. Rhodamine on its own fully penetrated in the biofilms (see Figure S1). Because all dendrons were synthesized to possess a single fluorescent rhodamine group, dendron distribution across the depth of the biofilms could be derived from the depth-dependent fluorescence intensity (Figure 2c,d) in the biofilm image, using a standard curve prepared using suspensions with known dendron concentrations (see Figure S2).

DOI: 10.1021/acs.nanolett.9b00838
Nano Lett. XXXX, XXX, XXX−XXX

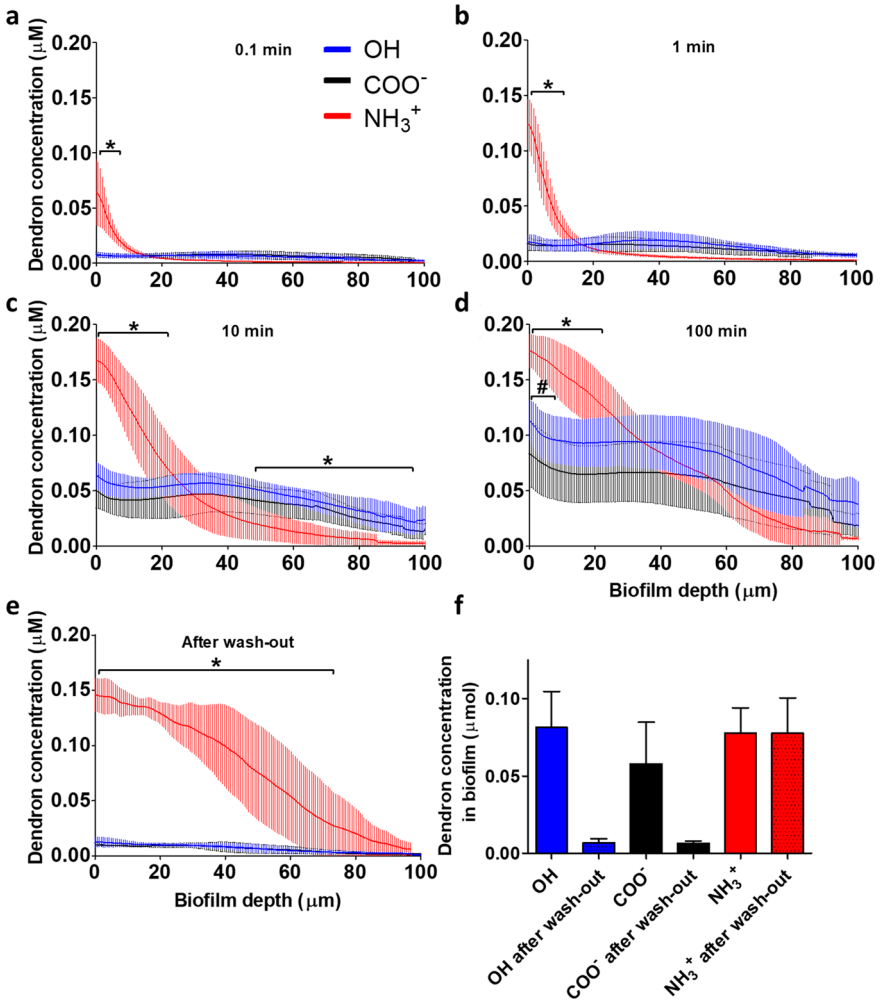

Figure 3. (a–d) Concentration of dendrons with different peripheral composition as a function of *P. aeruginosa* biofilm depth after exposure of biofilms to 0.2 μM dendron suspensions in PBS for 0.1, 1, 10, and 100 min (note black and blue data may be overlapping). (e) Concentration of dendrons in *P. aeruginosa* biofilms after 100 min exposure to a dendron suspension in PBS, followed by wash-out in PBS without dendrons for 100 min (note black and blue data are overlapping). (f) Total concentration of dendrons in *P. aeruginosa* biofilms after 100 min exposure to dendron suspensions and after subsequent wash-out for 100 min. Error bars denote standard deviations over six different biofilms, taken from different pans in three separate CDFF runs. Asterisks represent significant differences ($p < 0.05$; ANOVA with Tukey's posthoc analysis) between dendron periphery compositions: *, NH_3^+ versus COO^- and OH; #, COO^- versus OH.

Dendrons with NH_3^+ groups at their periphery accumulated faster into the acidic environment of *P. aeruginosa* biofilms than dendrons with OH or COO^- at their periphery (Figure 3a,b), mostly accumulating near the top of the biofilms. Although initially penetrating less than dendrons with NH_3^+ groups at their periphery, after 10 min exposure the accumulation of dendrons with OH and COO^- peripheral groups exceeded accumulation of dendrons with NH_3^+ peripheral groups in layers deeper than 30–40 μm into the biofilm (Figure 3c,d). Distribution of dendrons with OH and COO^- peripheral groups was more even across the depth of the biofilms than of dendrons with NH_3^+ groups at their periphery. Importantly, neither the distribution (Figure 3e) nor the total concentration (Figure 3f) of dendrons with NH_3^+ groups at their periphery was affected by exposure to PBS, whereas dendrons with OH or COO^- peripheral groups were largely washed-out during exposure to PBS.

Penetration and accumulation of antimicrobials, including antimicrobials transported by nanocarriers such as dendrimers, is a conditio sine qua non for effective bacterial killing in infectious biofilms. Most studies on antimicrobial nanoparticle penetration and accumulation in biofilms have focused on the effects of charge, but outcomes are indecisive. Negatively charged nanoparticles are generally said to penetrate more easily into biofilms[18−21] but oppositely also positively charged particles have been described to penetrate better into biofilms.[22] Penetration depends on (1) the availability of transportation channels in biofilms with sufficient width to allow nanocarrier passage, (2) diffusion coefficients of the nanocarriers depending on their configuration and composition, and (3) their interaction with the channel walls, that is, the EPS matrix or bacterial cell surfaces. Dendrons are extremely small in the order of 2–5 nm,[23] whereas water channel widths in biofilms are likely minimally 10-fold larger.[5] Thus, size differences between the dendrons applied and thus their diffusion coefficients can be excluded as being causative to the difference in penetration and accumulation observed between the three different dendrons. Unfortunately, their small size did not allow reliable measurement of their zeta potentials; however, based on their pH-responsive peripheral composition it can be assumed that within an acidic *P. aeruginosa* biofilm (pH around 6.5[24,25]) NH_3^+ groups (pK_a

DOI: 10.1021/acs.nanolett.9b00838
Nano Lett. XXXX, XXX, XXX−XXX

around 9) will be protonated and positively charged, whereas COO^- groups (pK_a around 2) are deprotonated and negatively charged. The OH groups will remain uncharged inside *P. aeruginosa* biofilms. At the same time, EPS components[26,27] and bacterial cell surfaces, including Pseudomonas ones,[28] remain negatively charged around pH 6.5. Thus, the accumulation of NH_3^+ dendrons near the top of a biofilm can be explained by strong, electrostatic double-layer mediated adhesion of dendrons, impeding their penetration to deeper biofilm layers. The OH and negatively charged COO^- dendrons will migrate deeper into the biofilms, as they experience no electrostatic double-layer attraction with the channel walls and utmost weak Lifshitz-van der Waals attraction. Therewith the deeper penetration of neutral and negatively charged particles goes at the expense of being easily washed-out, an aspect frequently neglected in the current literature. We here show that prevention of dendron wash-out critically depends on their peripheral composition, that is, positive charged groups.

Carefully engineered chemistries of biomaterials or drug carriers, including antimicrobial nanocarriers, can become compromised when applied in the human body through interaction with components in the blood, mucus, and extracellular matrix of human tissue. Because the current study was designed to provide basic knowledge about the interaction of dendrons with biofilm rather than demonstrate in vivo performance, experiments were done in a buffer. In a protein rich environment, proteins will adsorb on dendrons depending on their peripheral composition,[29] form a corona within 30 s, increase their hydrodynamic diameter, and make dendron zeta potentials less negative.[29] Yet,[22] surface-engineered nanoparticles possess the ability to permeate into cells,[30] tumors,[31] and pass the blood−brain barrier.[32] Smart micellar nanoparticles with adaptive, pH-responsive engineered surfaces maintained their surface-engineered properties to penetrate and accumulate in biofilms in vivo after transport through the blood.[22,33−38] This suggests maintenance of surface-engineered nanoparticle properties when applied under in vivo conditions. For more macroscopic biomaterials, it has been suggested[39] in the past that proteins adsorbed and adjusted their conformation in a way that is maintained to reflect the chemistry of the underlying material; however, whether such an argument is valid to explain the abilities of engineered nanoparticles in vivo remains to be demonstrated.

In conclusion, penetration and accumulation of dendrons into biofilms is controlled by their pH-responsive peripheral composition. This conclusion offers better understanding of interactions between dendrimers and biofilm components during penetration and accumulation that is important for the development of new antimicrobial dendritic nanocarriers but in addition also offers the perspective of controlling the accumulation depth of dendrimers inside a biofilm. Although the dendrons in this study were labeled with rhodamine as a tool to measure their penetration, rhodamine can easily be replaced with more therapeutically potent antimicrobials. Most antibiotics have a similar size as rhodamine and can be coupled to the focal point of the dendron, alike the rhodamine, through a hydrolyzable ester or disulfide bond, provided the antibiotics have a similar hydrophobicity. Subsequently, the dendron can control the penetration and accumulation into a biofilm according to its peripheral composition. Together with their good biocompatibility,[11] biodegradability,[12] and commercial availability, that is, often the biggest obstacle in downward clinical translation,[40] this warrants future exploitation of these dendrimers, as a new antimicrobial strategy for infection control.

Experimental Section. *Bacterial Strain, Growth Conditions, and Harvesting.* *P. aeruginosa* ATCC 39324, an isolate from a cystic fibrosis patient, was grown aerobically for 24 h at 37 °C on a blood agar plate from a frozen stock and stored at 4 °C until use. One single colony was added to 10 mL of tryptone soya broth (TSB, Oxoid, Basingstoke, United Kingdom) and grown for 24 h at 37 °C after which the broth was added to 200 mL of TSB and incubated 16 h under rotary shaking at 150 rpm (37 °C). Bacteria were harvested by centrifugation for 5 min at 5000*g*, after which the bacterial pellet was washed two times with PBS (PBS, 10 mM potassium phosphate, 150 mM sodium chloride, pH 7.0). Bacteria were suspended in 200 mL TSB at a concentration of 5×10^7 bacteria per mL, as determined using a Bürker-Türk counting chamber.

Biofilm Growth in the Constant Depth Film Fermenter. Biofilms were grown on stainless steel disks in the constant depth film fermenter (CDFF).[17] Sterile stainless steel disks (diameter 5 mm) were placed in a pan, equipped with five wells with adjustable depth to house five disks. Fifteen pans were placed in the turntable of the CDFF. The well-depth was set to allow growth of 100 μm thick biofilms with the aid of a scraper blade passing over each pan during rotation of the turntable at 3 rpm and maintaining the temperature inside the CDFF at 37 °C. For inoculation of the disks in the CDFF, 200 mL of bacterial suspension was dripped during 1 h on top of the pans, housing the disks. The turntable was stopped from revolving for 30 min, allowing the bacteria to adhere to the stainless steel disks, after which rotation was continued and artificial sputum medium[41] was dropwise added at a flow rate of 16 mL h^{-1} on top of the pans and scraped across. After 18 h of biofilm growth, disks with adhering biofilms were aseptically taken out of the pans. One CDFF run was comprised of 75 disks, from each run 15 randomly selected disk were taken from different pans for optical coherence tomography (OCT) analysis, and 30 biofilms were selected for dendron penetration experiments.

Optical Coherence Tomography. The thickness of biofilms was determined using OCT (Thorlabs Ganymade-II, Newton, NJ, U.S.A.). Biofilms were submerged in PBS, and three-dimensional scans of the complete biofilm were taken. OCT images were processed using a custom-made LabVIEW (National Instruments, Austin, TX, U.S.A.) script, which was corrected for background noise and possible tilting of the stainless steel disk surface. The average biofilm thickness was calculated using Otsu-thresholding of the image to determine the border between biofilm and surrounding fluid.[42]

Dendron Penetration in Biofilms and Cryo-Sectioning of Biofilms. Dendrons were suspended to a concentration of 0.2 μM in PBS and 20 μL of a dendron suspension was pipetted over a biofilm surface. Dendron suspensions were spread evenly over the entire surface of the biofilm. Biofilms were exposed to dendron suspensions for 0.1, 1, 10, or 100 min, after which the biofilms were dip-washed in PBS. In addition, biofilms exposed for 100 min to a suspension of dendrons in PBS were transferred to PBS without dendrons for another 100 min to monitor dendron wash-out. Directly after washing, biofilms were embedded in Tissue-Tek O.C.T. compound (Sakura Finetek Europe B.V., Alphen aan den Rijn, The Netherlands) and flash-frozen in liquid nitrogen. Next, biofilms

DOI: 10.1021/acs.nanolett.9b00838
Nano Lett. XXXX, XXX, XXX−XXX

were detached from their stainless-steel substratum for full embedding in Tissue-Tek and flash-freezing after which samples were stored in −80 °C until usage. Biofilms were cut in 10 μm thick sections using a cryotome (Leica CM3050 S, Leica Microsystems, Wetzlar, Germany) operating at −20 °C. Sections were collected on Menzel-Gläser superfrost slides (Thermo Fischer Scientific, Waltham, Massachusetts, U.S.A.) and kept in the dark until imaging, which was performed on the same day.

Fluorescent Imaging and Quantification of Dendron Penetration and Accumulation. Fluorescence microscopy (Leica DM 4000 B, Leica Microsystems Heidelberg Gmbh, Heidelberg, Germany) was carried out to image the biofilm sections. Fluorescence images were analyzed using a custom-built LabVIEW script to obtain the red-fluorescence intensity along the biofilm depth (see Figure 2c). The LabVIEW script first divided the biofilm image in vertical columns of 0.645 μm width (covering 1 pixel). Then, it aligned all the vertical columns with their tops along a straight line, after which the script calculated the average intensity profile as a function of biofilm depth. The dendron concentration in the biofilm was derived from the fluorescence intensity with a standard curve (Figure S2).

■ ASSOCIATED CONTENT

Supporting Information

The Supporting Information is available free of charge on the ACS Publications website at DOI: 10.1021/acs.nanolett.9b00838.

Light- and fluorescence micrographs of rhodamine penetration into a 100 μm thick *P. aeruginosa* ATCC 39324 biofilm; synthesis of dendrons with different, pH-responsive peripheral compositions, calibration curves relating the fluorescent intensities to dendron concentration (PDF)

■ AUTHOR INFORMATION

Corresponding Authors

*(P.S.) E-mail: p.k.sharma@umcg.nl. Phone: +31503616097.
*(M.M.) E-mail: malkoch@kth.se. Phone: +4687908768.

ORCID

Henny C. van der Mei: 0000-0003-0760-8900
Michael Malkoch: 0000-0002-9200-8004
Prashant K. Sharma: 0000-0002-8342-8939

Notes

The authors declare the following competing financial interest(s): H.J.B. is also director of a consulting company, SASA BV (GN Schutterlaan 4, 9797 PC Thesinge, The Netherlands). The authors declare no potential conflicts of interest with respect to authorship and/or publication of this article. Opinions and assertions contained herein are those of the authors and are not construed as necessarily representing views of their respective employers.

■ ACKNOWLEDGMENTS

The research leading to these results has received funding from the European Union's Seventh Framework Program (FP7/2007-2013) under Grant Agreement 604182, http://ec.europa.eu.research. It was carried out within the project FORMAMP, Innovative Nanoformulation of Antimicrobial Peptides to Treat Bacterial Infectious Diseases. Polymer Factory Sweden AB is acknowledged for its support in the synthesis of the dendrons utilized in this project and as partners in FORMAMP.

■ REFERENCES

(1) Fux, C. A.; Costerton, J. W.; Stewart, P. S.; Stoodley, P. Survival Strategies of Infectious Biofilms. *Trends Microbiol.* **2005**, *13* (1), 34−40.

(2) Ciofu, O.; Tolker-Nielsen, T.; Jensen, P. Ø.; Wang, H.; Høiby, N. Antimicrobial Resistance, Respiratory Tract Infections and Role of Biofilms in Lung Infections in Cystic Fibrosis Patients. *Adv. Drug Delivery Rev.* **2015**, *85*, 7−23.

(3) Van Leeuwhoek, A. An Abstract of a Letter from Mr. Anthony Leevvenhoeck at Delft, Dated Sep. 17. 1683. Containing Some Microscopical Observations, about Animals in the Scurf of the Teeth, the Substance Call'd Worms in the Nose, the Cuticula Consisting of Scales. *Philos. Trans. R. Soc.* **1684**, *14*, 575−582.

(4) Humphreys, G.; Fleck, F. United Nations Meeting on Antimicrobial Resistance. *Bull. World Health Organ.* **2016**, *94* (9), 638−639.

(5) Liu, Y.; Shi, L.; Su, L.; Van der Mei, H. C.; Jutte, P. C.; Ren, Y.; Busscher, H. J. Nanotechnology-Based Antimicrobials and Delivery Systems for Biofilm-Infection Control. *Chem. Soc. Rev.* **2019**, *48*, 428−446.

(6) Lam, S. J.; O'Brien-Simpson, N. M.; Pantarat, N.; Sulistio, A.; Wong, E. H. H.; Chen, Y. Y.; Lenzo, J. C.; Holden, J. A.; Blencowe, A.; Reynolds, E. C.; et al. Combating Multidrug-Resistant Gram-Negative Bacteria with Structurally Nanoengineered Antimicrobial Peptide Polymers. *Nat. Microbiol.* **2016**, *1*, 1−11.

(7) Reymond, J. L.; Bergmann, M.; Darbre, T. Glycopeptide Dendrimers as *Pseudomonas aeruginosa* Biofilm Inhibitors. *Chem. Soc. Rev.* **2013**, *42* (11), 4814−4822.

(8) Choi, S. K.; Myc, A.; Silpe, J. E.; Sumit, M.; Wong, P. T.; McCarthy, K.; Desai, A. M.; Thomas, T. P.; Kotlyar, A.; Holl, M. M. B.; et al. Dendrimer-Based Multivalent Vancomycin Nanoplatform for Targeting the Drug-Resistant Bacterial Surface. *ACS Nano* **2013**, *7* (1), 214−228.

(9) Carlmark, A.; Hawker, C.; Hult, A.; Malkoch, M. New Methodologies in the Construction of Dendritic Materials. *Chem. Soc. Rev.* **2009**, *38* (2), 352−362.

(10) Lyczak, J. B.; Cannon, C. L.; Pier, G. B. Establishment of *Pseudomonas aeruginosa* Infection: Lessons from a Versatile Opportunist. *Microbes Infect.* **2000**, *2* (9), 1051−1060.

(11) Carlmark, A.; Malmström, E.; Malkoch, M. Dendritic Architectures Based on Bis-MPA: Functional Polymeric Scaffolds for Application-Driven Research. *Chem. Soc. Rev.* **2013**, *42* (13), 5858−5879.

(12) Feliu, N.; Walter, M. V.; Montañez, M. I.; Kunzmann, A.; Hult, A.; Nyström, A.; Malkoch, M.; Fadeel, B. Stability and Biocompatibility of a Library of Polyester Dendrimers in Comparison to Polyamidoamine Dendrimers. *Biomaterials* **2012**, *33* (7), 1970−1981.

(13) Walter, M. V.; Malkoch, M. Simplifying the Synthesis of Dendrimers: Accelerated Approaches. *Chem. Soc. Rev.* **2012**, *41* (13), 4593−4722.

(14) García-Gallego, S.; Hult, D.; Olsson, J. V.; Malkoch, M. Fluoride-Promoted Esterification with Imidazolide-Activated Compounds: A Modular and Sustainable Approach to Dendrimers. *Angew. Chem.* **2015**, *127*, 2446−2449.

(15) Stenström, P.; Andrén, O. C. J.; Malkoch, M. Fluoride-Promoted Esterification (FPE) Chemistry: A Robust Route to Bis-MPA Dendrons and Their Postfunctionalization. *Molecules* **2016**, *21* (3), 366.

(16) García-Gallego, S.; Nyström, A. M.; Malkoch, M. Chemistry of Multifunctional Polymers Based on Bis-MPA and Their Cutting-Edge Applications. *Prog. Polym. Sci.* **2015**, *48*, 85−110.

(17) Rozenbaum, R. T.; Woudstra, W.; de Jong, E. D.; Van der Mei, H. C.; Busscher, H. J.; Sharma, P. K. A Constant Depth Film

DOI: 10.1021/acs.nanolett.9b00838
Nano Lett. XXXX, XXX, XXX−XXX

Fermenter to Grow Microbial Biofilms. *Nat. Protoc. Exch.* **2017**, DOI: 10.1038/protex.2017.024.
(18) Peulen, T.-O.; Wilkinson, K. J. Diffusion of Nanoparticles in a Biofilm. *Environ. Sci. Technol.* **2011**, *45*, 3367−3373.
(19) Guiot, E.; Georges, P.; Brun, A.; Fontaine-Aupart, M. P.; Bellon-Fontaine, M. N.; Briandet, R. Heterogeneity of Diffusion inside Microbial Biofilms Determined by Fluorescence Correlation Spectroscopy under Two-Photon Excitation. *Photochem. Photobiol.* **2002**, *75* (6), 570−578.
(20) Nevius, B. A.; Chen, Y. P.; Ferry, J. L.; Decho, A. W. Surface-Functionalization Effects on Uptake of Fluorescent Polystyrene Nanoparticles by Model Biofilms. *Ecotoxicology* **2012**, *21* (8), 2205−2213.
(21) Liu, Y.; Busscher, H. J.; Zhao, B.; Li, Y.; Zhang, Z.; Van der Mei, H. C.; Ren, Y.; Shi, L. Surface-Adaptive, Antimicrobially Loaded, Micellar Nanocarriers with Enhanced Penetration and Killing Efficiency in Staphylococcal Biofilms. *ACS Nano* **2016**, *10* (4), 4779−4789.
(22) Li, X.; Yeh, Y.-C.; Giri, K.; Mout, R.; Landis, R. F.; Prakash, Y. S.; Rotello, V. M. Control of Nanoparticle Penetration into Biofilms through Surface Design. *Chem. Commun.* **2015**, *51* (2), 282−285.
(23) Dobrovolskaia, M. A.; Patri, A. K.; Simak, J.; Hall, J. B.; Semberova, J.; Lacerda, S. H. D. P.; Mcneil, S. E. Nanoparticle Size and Surface Charge Determine Effects of PAMAM Dendrimers on Human Platelets *in Vitro*. *Mol. Pharmaceutics* **2011**, *9* (3), 382−393.
(24) Hunter, R. C.; Beveridge, T. J. Application of a PH-Sensitive Fluoroprobe (C-SNARF-4) for PH Microenvironment Analysis in *Pseudomonas aeruginosa* Biofilms. *Appl. Environ. Microbiol.* **2005**, *71* (5), 2501−2510.
(25) Wilton, M.; Charron-Mazenod, L.; Moore, R.; Lewenza, S. Extracellular DNA Acidifies Biofilms and Induces Aminoglycoside Resistance in *Pseudomonas aeruginosa*. *Antimicrob. Agents Chemother.* **2016**, *60* (1), 544−553.
(26) Chiang, W. C.; Nilsson, M.; Jensen, P. Ø.; Høiby, N.; Nielsen, T. E.; Givskov, M.; Tolker-Nielsen, T. Extracellular DNA Shields against Aminoglycosides in *Pseudomonas aeruginosa* Biofilms. *Antimicrob. Agents Chemother.* **2013**, *57* (5), 2352−2361.
(27) Nichols, W. W.; Dorrington, S. M.; Slack, M. P. E.; Walmsley, H. L. Inhibition of Tobramycin Diffusion by Binding to Alginate. *Antimicrob. Agents Chemother.* **1988**, *32* (4), 518−523.
(28) Roosjen, A.; Busscher, H. J.; Norde, W.; van der Mei, H. C. Bacterial Factors Influencing Adhesion of *Pseudomonas aeruginosa* Strains to a Poly(Ethylene Oxide) Brush. *Microbiology* **2006**, *152* (9), 2673−2682.
(29) Tenzer, S.; Docter, D.; Kuharev, J.; Musyanovych, A.; Fetz, V.; Hecht, R.; Schlenk, F.; Fischer, D.; Kiouptsi, K.; Reinhardt, C.; et al. Rapid Formation of Plasma Protein Corona Critically Affects Nanoparticle Pathophysiology. *Nat. Nanotechnol.* **2013**, *8* (10), 772−781.
(30) Slowing, I. I.; Vivero-Escoto, J. L.; Wu, C. W.; Lin, V. S. Y. Mesoporous Silica Nanoparticles as Controlled Release Drug Delivery and Gene Transfection Carriers. *Adv. Drug Delivery Rev.* **2008**, *60* (11), 1278−1288.
(31) Kim, B.; Han, G.; Toley, B. J.; Kim, C.-K.; Rotello, V. M.; Forbes, N. S. Tuning Payload Delivery in Tumour Cylindroids Using Gold Nanoparticles. *Nat. Nanotechnol.* **2010**, *5* (6), 465−472.
(32) Lockman, P. R.; Mumper, R. J.; Khan, M. A.; Allen, D. D.; Mumper, R. J.; Khan, M. A.; Allen, D. D. Nanoparticle Technology for Drug Delivery Across the Blood-Brain Barrier Nanoparticle Technology for Drug Delivery Across the Blood-Brain Barrier. *Drug Dev. Ind. Pharm.* **2002**, *28* (1), 1−13.
(33) Aldeek, F.; Balan, L.; Medjahdi, G.; Roques-Carmes, T.; Malval, J. P.; Mustin, C.; Ghanbaja, J.; Schneider, R. Enhanced Optical Properties of Core/Shell/Shell CdTe/CdS/ZnO Quantum Dots Prepared in Aqueous Solution. *J. Phys. Chem. C* **2009**, *113* (45), 19458−19467.
(34) Aldeek, F.; Mustin, C.; Balan, L.; Medjahdi, G.; Roques-Carmes, T.; Arnoux, P.; Schneider, R. Enhanced Photostability from CdSe(S)/ZnO Core/Shell Quantum Dots and Their Use in Biolabeling. *Eur. J. Inorg. Chem.* **2011**, *2011*, 794−801.
(35) Aldeek, F.; Schneider, R.; Fontaine-Aupart, M.-P.; Mustin, C.; Lécart, S.; Merlin, C.; Block, J.-C. Patterned Hydrophobic Domains in the Exopolymer Matrix of MR-1 Biofilms. *Appl. Environ. Microbiol.* **2013**, *79* (4), 1400−1402.
(36) Aldeek, F.; Mustin, C.; Balan, L.; Roques-carmes, T.; Fontaine-aupart, M.; Schneider, R. Biomaterials Surface-Engineered Quantum Dots for the Labeling of Hydrophobic Microdomains in Bacterial Bio Fi Lms. *Biomaterials* **2011**, *32* (23), 5459−5470.
(37) Morrow, J. B.; Arango, C. P.; Holbrook, R. D. Association of Quantum Dot Nanoparticles with *Pseudomonas aeruginosa* Biofilm. *J. Environ. Qual.* **2010**, *39*, 1934−1941.
(38) Chalmers, N. I.; Palmer, R. J.; Du-thumm, L.; Sullivan, R.; Shi, W.; Kolenbrander, P. E. Use of Quantum Dot Luminescent Probes To Achieve Single-Cell Resolution of Human Oral Bacteria in Biofilms. *Appl. Environ. Microbiol.* **2007**, *73* (2), 630−636.
(39) Schakenraad, J. M.; Busscher, H. J. Cell-Polymer Interactions : Protein Adsorption The Influence Of. *Colloids Surf.* **1989**, *42*, 331−343.
(40) Busscher, H. J.; Alt, V.; Van der Mei, H. C.; Fagette, P.; Zimmerli, W.; Moriarty, T. F.; Parvizi, J.; Schmidmaier, G.; Raschke, M.; Gehrke, T.; et al. A Trans-Atlantic Perspective on Stagnation in Clinical Translation of Antimicrobial Strategies for the Control of Biomaterial-Implant Associated Infection. *ACS Biomater. Sci. Eng.* **2019**, *5*, 402−406.
(41) Sriramulu, D. D.; Lu, H.; Lam, J. S. Microcolony Formation: A Novel Biofilm Model of *Pseudomonas aeruginosa* for the Cystic Fibrosis Lung. *J. Med. Microbiol.* **2005**, *54*, 667−676.
(42) Hou, J.; Veeregowda, D. H.; van de Belt-Gritter, B.; Busscher, H. J.; van der Mei, H. C. Extracellular Polymeric Matrix Production and Relaxation under Fluid Shear and Mechanical Pressure in *Staphylococcus aureus* Biofilms. *Appl. Environ. Microbiol.* **2018**, *84* (1), 1−14.

DOI: 10.1021/acs.nanolett.9b00838
Nano Lett. XXXX, XXX, XXX−XXX